Dynamic Systems and Applications 32 (2023) 199-229

LARCH BUDMOTH INTERACTION: STABILITY, BIFURCATION AND CHAOS CONTROL

E. M. ELSAYED[1] AND QAMAR DIN[2]

[1]Department of Mathematics, Faculty of Science, King Abdulaziz University, Jeddah 21589, Saudi Arabia, and Department of Mathematics, Faculty of Science, Mansoura University, Mansoura 35516, Egypt.
E-mail: emmelsayed@yahoo.com.

[2]Department of Mathematics, University of Poonch Rawalakot, Rawalakot 12350, Pakistan. E-mail: qdin78@hotmail.com.

ABSTRACT. Taking into account the interaction between budmoth and quality of larch trees located in the Swiss Alps (a mountain range in Switzerland), a discrete-time model is proposed and studied. The novel model is proposed with implementation of Holling type III functional response for interaction of plant quality. The proposed functional response is validated with real observed data of larch budmoth interaction. Furthermore, we investigate qualitative behavior of this proposed discrete-time system for interaction between budmoth and quality of larch trees. Boundedness of solutions, existence of fixed points and their local behavior is carried out. It is proved that system experiences period-doubling bifurcation at its positive fixed point with utilizing center manifold theorem and normal forms theory. Moreover, existence and direction for Neimark-Sacker bifurcation are also investigated for larch budmoth interaction. Bifurcating and fluctuating behaviors of system are controlled through utilization of chaos control strategies. Numerical simulations are presented to demonstrate the theoretical findings. At the end, theoretical investigations are validated with field and experimental data.

AMS (MOS) Subject Classification. 39A30, 40A05, 92D25,92C50.

Key Words and Phrases. Larch budmoth interaction; stability; period-doubling bifurcation; Neimark-Sacker bifurcation; chaos control.

1. Introduction and mathematical model

Ecologists argue that small mammals with their consumers and forest insects are two main classes of animals which have population dynamics of cyclic type. Lepidoptera from moderate zonal are most prominent insects of such type [1]. According

Received June 3, 2023 ISSN 1056-2176(Print); ISSN 2693-5295 (online)
www.dynamicpublishers.org https://doi.org/10.46719/dsa2023.32.12

to Myers [2], oscillations occur in population densities of 18 species of budmoth. Resolving the reasons of such periodic oscillations is an important topic for both practical and theoretical researchers. The larch budmoth interaction is one of the population cycles of classical type. Experiments show that density of budmoth changes by approximately fifth order of magnitude, whereas amplitude and period remain remarkably constant. The interaction between budmoth and larch trees, supply of its food and needles of larch, is a topic of great interest and many researchers are attracted by this field for the last few decades. This population cycle is described as resource-consumer interaction, in which larch needles behave like a source and budmoth is considered as consumer. The high-quality needles of larch trees are badly affected due to outbreaks of budmoth, and in a result low-quality leaves are produced for the next year. Ultimately, the length of needles remains shorter with higher raw quantity of fiber. Feeding on these affected needles gives less larval survival chance and female fertility. Several years can take for the improvement of leaves quality. Mathematical models related to these larch budmoth interaction can produce cycles with great resemblance to observed data. Larch budmoth is a worm of grey color which became famous for its periodic behavior of outbreaks and infestations on large-scale with larch trees located in Alpine valleys of Europe. For further description related to biology of larch budmoth, their natural enemies, their population cycles, reconstruction of historical cycles, reasons behinds the creation of cycles, negative feedback of needle quality, regulation by natural enemies, fitness of various ecotypes, migration of moth and dispersal, cycles in the nutshell, variation of cycles with respect to climate change, importance of larch budmoth, possible sources of confusion and control measures, the interested readers are referred to recently published article [3]. The interaction related to larch budmoth reveals rich dynamics such as complexity, fluctuating and chaotic behavior [4]. Moreover, cycles of larch budmoth population interaction have been reported by many researchers (cf. [5, 6, 7, 8, 9, 10, 11]). Due to seasonal variation (non-overlapping generations) in the interaction related to larch budmoth, it is more appropriate to model such interaction with discrete-time systems of host-parasitoid type. Such mathematical framework allows us to explore qualitative behavior of these models. Jang and Johnson in [12] investigated one model related to leaf quality-moth interaction and two moth-parasitoid systems. They discussed stability, existence of equilibria, persistence and period-doubling bifurcation for these discrete models. Jang and Yu in [13] studied one simple system related to plant quality-moth interaction and other model with implementation of Ricker equation. They also explored presence of Neimark-Sacker bifurcation for the model with Ricker type growth function. In [14], De Silva and Jang considered model of larch budmoth interaction. The original model was proposed in [11], and authors of [14] used an approximation in moth equation. With this approximation, they showed persistence of solutions, existence

of fixed points, their stability and bifurcations of two types, that is, Neimark-Sacker bifurcation and period-doubling bifurcation. Iyengar et al. [15] investigated impact of climate change on the interaction of larch budmoth system. In order to give an explanation for the irregular larch budmoth cyclic outbreaks observed in the French Alps, Balakrishnan et al. [16] proposed important modifications in models related to larch budmoth interaction by implementing a slow time dependence in one of the species–specific parameters. Taking into account the interaction between plant quality and larch budmoth in Swiss Apls, recently Ali et al. [17] reported period-doubling bifurcation, Neimark-Sacker bifurcation and chaos control for a class of discrete-time system with Ricker equation.

Arguing as in [11], assume that x_n represents larch budmoth density at time n, where $n = 0, 1, 2, \cdots$. On the other hand, as foliage of larch tree is eaten by the budmoth, the fluctuations are observed in their nutritive content and biomass. The quality of leaf at time n is represented by y_n, and it can be expressed in terms of needle length z_n as follows:

$$y_{n+1} = (z_n - 15\,mm)/15\,mm,$$

where z_n the needle length index changes such that $z_n \in [15\,mm,\ 30\,mm]$.

Keeping in view the interaction between leaf quality and larch budmoth population, a two-dimensional model is given as follows:

$$\begin{aligned} x_{n+1} &= x_n \exp\left(r\,\left(1 - \exp\left(-\frac{y_n}{a}\right)\right) - \frac{r}{k}\,x_n\right), \\ y_{n+1} &= (1-b) + by_n - \frac{cx_n}{d + x_n}, \end{aligned} \tag{1.1}$$

where all parameters are positive and $b < 1$. Assume that $F(y) := 1 - \exp\left(-\frac{y}{a}\right)$, then a linear approximation of $F(y)$ is used in [14] as follows:

$$1 - \exp\left(-\frac{y}{a}\right) \approx \frac{y}{a}.$$

Fig. 1 shows that linear approximation for $F(y)$ is not appropriate with its exact value. Therefore, it is suitable to implement some nonlinear approximation for $F(y)$. In this paper, we discuss dynamics of system (1.1) with the following more appropriate nonlinear approximation for $F(y)$:

$$1 - \exp\left(-\frac{y}{a}\right) \approx \frac{y^2}{a + y^2} := G(y).$$

With implementation of nonlinear approximation $G(y)$, system (1.1) is approximated as follows:

$$\begin{aligned} x_{n+1} &= x_n \exp\left(r\,\left(\frac{y_n^2}{a + y_n^2}\right) - \frac{r}{k}\,x_n\right), \\ y_{n+1} &= (1-b) + by_n - \frac{cx_n}{d + x_n}. \end{aligned} \tag{1.2}$$

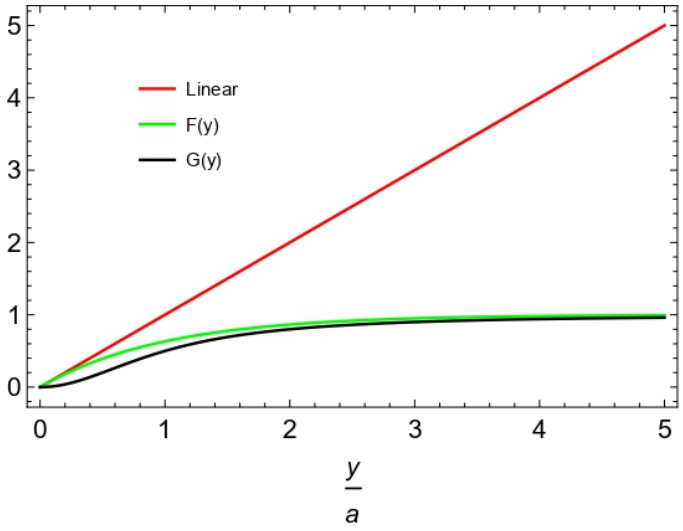

FIGURE 1. Comparison of $F(y)$, $G(y)$ and linear approximation $\frac{y}{a}$.

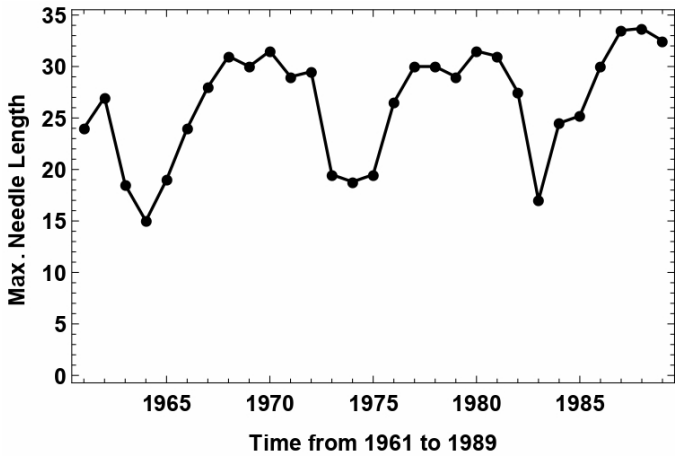

FIGURE 2. Variation in maximum needle length (in mm) from 1961 to 1989.

Next, in order to validate the proposed functional response $G(y) = \frac{y^2}{a+y^2}$ with real observed data of larch budmoth interaction, we consider the data reported by Baltensweiler *et al.* [18] in Engadine (Switzerland). According to their study, the maximum change in needle length starting from year 1961 to year 1989 is depicted in Fig. 2. In Fig. 2, the minimum length of needle is recorded as $15\,mm$, whereas the maximum length of needle is $33.7\,mm$. Therefore, the quality of leaf y_n at time n is expressed in terms of needle length z_n as follows:

$$y_{n+1} = (z_n - 15\,mm)/18.7\,mm.$$

Using nonlinear regression analysis, the observed data from 1961 to 1989 for maximum needle length index with proposed functional response $G(y) = \frac{y^2}{a+y^2}$ is fitted. The best fitted value for parameter a is investigated as $a = 88.1367$, whereas the parameter

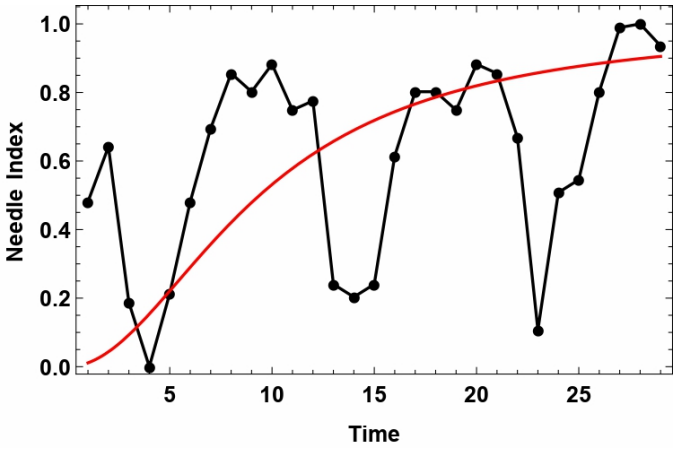

FIGURE 3. Variation in maximum needle length index and fitted functional response $G(y)$.

confidence interval is $[26.3846, 149.889]$ with 95 percent confidence level. On the other hand, taking into account $F(y)$ we have $a = 14.2143$ the best fitted value and the parameter confidence interval is $[9.13824, 19.2905]$ with 95 percent confidence level. Keeping in view the linear functional response, $a = 29.0379$ is the best fitted value and $[22.911, 35.1648]$ is confidence interval with 95 percent confidence level. Consequently, more reasonable confidence interval is obtained in case of $G(y)$. The variation in maximum needle length index from 1961 to 1989 and fitted proposed functional response $G(y) = \frac{y^2}{a+y^2}$ are depicted in Fig. 3. Moreover, according to study of [3], cyclical population fluctuations of the larch budmoth were observed in the Upper Engadine with mean periodicity was 8.5 years, and at the peak of an outbreak, there were more than twenty thousand larvae on a single larch tree, which concludes that consumers (predators) are much bigger than their resources (preys). Hassell *et al.* [19] argued that Holling type III functional response should be particularly common in predators that are much bigger than their prey. Taking into account the study of [3, 19], and aforementioned nonlinear regression analysis, it is more appropriate to implement Holling type III functional response (that is, $G(y)$) instead of Ivlev type functional response (that is, $F(y)$) for the plant quality index.

Furthermore, biological meanings of parametric values of system (1.2) are presented in Table 1.

The motivational aspects and novelty of this paper are further described as follows:

- A novel discrete model for interaction between larch budmoth and plant quality is proposed and studied.
- The proposed model is more appropriate for mathematical analysis and validated with observed data.

Parameter value	Biological meaning of parameter
r	larch budmoth growth rate
a	reciprocal of speed of convergence of leaf quality to its maximum value
k	inverse intraspecific competition coefficient of larch budmoth
b	plant unprotectedness
c	maximal uptake rate of moth
d	half saturation constant of moth grazing rate

TABLE 1. Biological meanings of parameters of system (1.2).

- The proposed system undergoes Neimark-Sacker bifurcation and period-doubling bifurcation about its interior fixed point whenever growth rate of consumer is selected as bifurcation parameter.
- Hybrid and exponential type chaos control methods are applied to proposed system (1.2).

We summarize the remaining discussion of this paper as follows. Boundedness of solutions for system (1.2), existence of biologically feasible equilibria, and conditions for local asymptotic stability of these equilibria are investigated in Section 2. In Section 3, we show that interior equilibrium of system (1.2) undergoes period-doubling bifurcation whenever growth parameter r of larch budmoth population is taken as bifurcation parameter. In Section 4, it is proved that system (1.2) undergoes Neimark-Sacker bifurcation around its interior equilibrium point. OGY and hybrid control methods are introduced in Section 5. Lastly, numerical simulations are provided in Section 7 to illustrate our theoretical discussion.

2. **Boundedness and existence of equilibria**

In this section, first we show that every solution $\{(x_n, y_n)\}$ of system (1.2) is uniformly bounded. For this, the following Lemma is presented.

Lemma 2.1. [20] *Assume that* η_n *satisfies* $\eta_{n+1} \leq \eta_n \exp(\alpha(1-\beta\eta_n))$ *for all* $n \in [n_1, \infty)$ *with* $\eta_0 > 0$, *where* $\alpha,\ \beta > 0$. *Then,* $\limsup_{n\to\infty} \eta_n \leq \frac{1}{\alpha\beta}\exp(\alpha-1)$.

Lemma 2.2. *Every solution* $\{(x_n, y_n)\}$ *of system* (1.2) *is uniformly bounded.*

Proof. Suppose that $x_0 > 0$ and $y_0 > 0$, then every solution $\{(x_n, y_n)\}$ of the system (1.2) satisfies $x_n > 0$ and $y_n > 0$ for all $n \geq 0$. First, keeping in view positivity of solutions of system (1.2) and from second equation of system (1.2) it follows that $y_{n+1} \leq (1-b) + by_n$. Then, comparison argument yields that $\limsup_{n\to\infty} y_n \leq 1$. Next, taking into account the positivity of solutions of system (1.2) and considering the first

equation of the system (1.2) we have

$$\begin{aligned} x_{n+1} &= x_n \exp\left(r\left(\frac{y_n^2}{a+y_n^2}\right) - \frac{r}{k}x_n\right) \\ &\leq x_n \exp\left(r\left(\frac{y_n^2}{a} - \frac{1}{k}x_n\right)\right) \\ &\leq x_n \exp\left(r\left(\frac{1}{a} - \frac{1}{k}x_n\right)\right) \\ &= x_n \exp\left(\frac{r}{a}\left(1 - \frac{a}{k}x_n\right)\right). \end{aligned}$$

Next, an application of Lemma 2.1 yields that

$$\lim_{n\to\infty} \sup x_n \leq \frac{k}{r}\exp\left(\frac{r}{a} - 1\right).$$

□

With mathematical induction one can prove the following result.

Lemma 2.3. *Assume that* $0 < x_0 \leq \frac{k}{r}\exp\left(\frac{r}{a} - 1\right)$ *and* $0 < y_0 \leq 1$*, then the rectangle* $\left[0, \frac{k}{r}\exp\left(\frac{r}{a} - 1\right)\right] \times [0, 1]$ *is invariant interval for every positive solution* $\{(x_n, y_n)\}$ *of the system* (1.2)*.*

Secondly, we explore the biologically feasible fixed points of system (1.2). The steady-states of system (1.2) satisfy the following two-dimensional algebraic equations:

$$\begin{aligned} x &= x\exp\left(r\left(\frac{y^2}{a+y^2}\right) - \frac{r}{k}x\right), \\ y &= 1 - b + by - \frac{cx}{d+x}. \end{aligned} \tag{2.1}$$

Then, it is quite easy to see that $E = (0, 1)$ is boundary equilibrium of (1.2). We are interested in interior equilibrium of system (1.2) in closed form. Neglecting the boundary solution of system (2.1), we left with the following algebraic system for coexistence:

$$\begin{aligned} (k-x)y^2 - ax &= 0, \\ y &= 1 - b + by - \frac{cx}{d+x}. \end{aligned} \tag{2.2}$$

From (2.2), it follows that positive fixed point (x^*, y^*) of system (1.2) satisfies:

$$y^* := 1 - \frac{c\,x^*}{(1-b)(d+x^*)},$$

where x^* is a positive real root for the following cubic equation:

$$\alpha x^3 + \beta x^2 + \gamma x + \delta = 0, \tag{2.3}$$

where

$$\alpha := (1+a)(b+c-1)^2,$$

$$\beta := (b+c-1)(2(a+1)(b-1)d - k(b+c)+k),$$
$$\gamma := (b-1)d((a+1)(b-1)d - 2k(b+c-1)),$$

and

$$\delta := -(1-b)^2 d^2 k.$$

Moreover, the following Lemma gives the conditions for existence of unique positive root for cubic Eq. (2.3).

Lemma 2.4. *Assume that $b+c \neq 1$, then Eq. (2.3) has unique positive root if $\Delta < 0$, where*

$$\Delta := 18\alpha\beta\gamma\delta - 4\beta^3\delta + \beta^2\gamma^2 - 4\alpha\gamma^3 - 27\alpha^2\delta^2. \tag{2.4}$$

Proof. Taking $P(x) = \alpha x^3 + \beta x^2 + \gamma x + \delta$, and assume that $b+c \neq 1$, then it follows that $P(0) = -(1-b)^2 d^2 k < 0$ and $\lim_{x\to\infty} P(x) = +\infty$. Therefore, according to the intermediate value property of continuous functions, $P(x)$ has at least one positive solution. Furthermore, assume that $\Delta < 0$, then according to Descartes' rule of signs, $P(x)$ has unique positive real root. □

Taking into account Lemma 2.4, one has the following result for existence of unique positive equilibrium point of system (1.2).

Lemma 2.5. *Assume that $b+c > 1$ and $\Delta < 0$, then there exists unique positive equilibrium point (x^*, y^*) for system (1.2) satisfying $0 < y^* < 1$ and $0 < x^* < \frac{d(1-b)}{b+c-1}$.*

Moreover, existence of interior (positive) fixed point (x^*, y^*) can be shown by method of isoclines. These isoclines satisfy the following equation:

$$\Psi_1(x) = \Psi_2(x),$$

where

$$\Psi_1(x) := \sqrt{\frac{ax}{k-x}},$$

and

$$\Psi_2(x) := 1 - \frac{c\,x}{(1-b)(d+x)}.$$

The existence of unique positive fixed point is depicted in Fig. 4. Next, we check local dynamics for equilibria of system (1.2). For this, first taking into account the boundary equilibrium, it is easy to see that the Jacobian matrix of (1.2) at boundary equilibrium E is given by:

$$J(E) = \begin{pmatrix} e^{\frac{r}{1+a}} & 0 \\ -\frac{c}{d} & b \end{pmatrix}.$$

Then, eigenvalues of $J(E)$ are $\mu_1 = e^{\frac{r}{a+1}} > 1$ and $\mu_2 = b < 1$. Therefore, E is a saddle point.

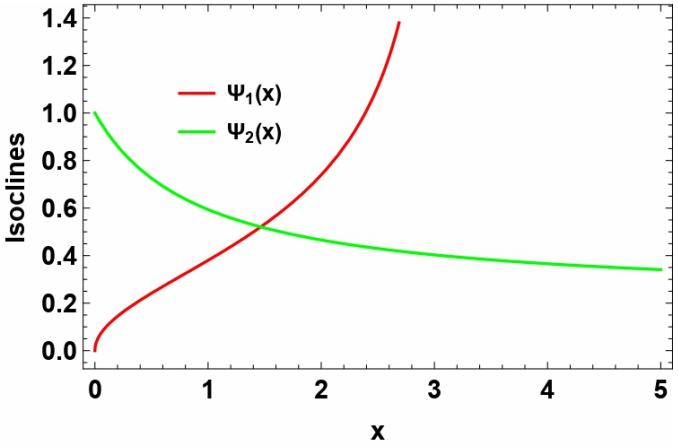

FIGURE 4. Existence of unique positive fixed point.

Secondly, it is easy to see that the Jacobian matrix of (1.2) at interior equilibrium $P = (x^*, y^*)$ is given by:

$$J(P) = \begin{pmatrix} \frac{k-rx^*}{k} & \frac{2arx^*y^*}{(a+y^{*2})^2} \\ -\frac{cd}{(c+x^*)^2} & b \end{pmatrix}. \tag{2.5}$$

Now characteristic polynomial of $J(P)$ is given by:

$$F(\mu) = \mu^2 - \left(b + \frac{k-rx^*}{k}\right)\mu + b + \frac{2acdrx^*y^*}{(a+y^{*2})^2(d+x^*)^2} - \frac{brx^*}{k}. \tag{2.6}$$

From (2.6), it follows that

$$F(1) = rx^*\left(\frac{2acdy^*}{(a+y^{*2})^2(d+x^*)^2} + \frac{1-b}{k}\right) > 0.$$

Furthermore, the following Lemma gives local dynamical behavior of system (1.2) at its positive fixed point.

Lemma 2.6. *The following results hold true for system* (1.2)*:*

(i) The positive equilibrium (x^*, y^*) *is a sink if and only if*

$$\frac{2acdrx^*y^*}{(a+y^{*2})^2(d+x^*)^2} + \frac{(b+1)(2k-rx^*)}{k} > 0,$$

and

$$b + \frac{2acdrx^*y^*}{(a+y^{*2})^2(d+x^*)^2} - \frac{brx^*}{k} < 1.$$

(ii) The positive equilibrium (x^*, y^*) *is a saddle point if and only if*

$$\frac{2acdrx^*y^*}{(a+y^{*2})^2(d+x^*)^2} + \frac{(b+1)(2k-rx^*)}{k} < 0.$$

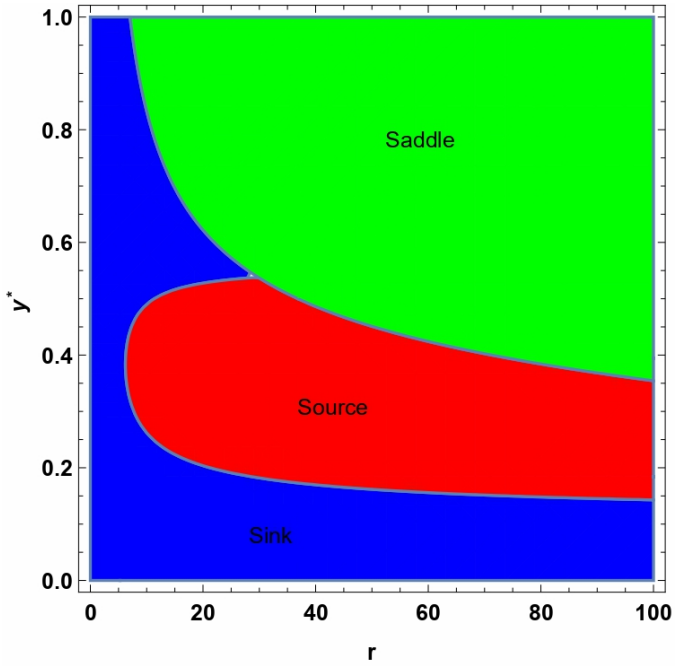

FIGURE 5. Phase-plane analysis of (x^*, y^*) with $a = 1.95$, $c = 1.1$, $d = 35$, $k = 255$ and $b = 0.85$ in ry^*-plane.

(iii) The positive equilibrium (x^*, y^*) is a source if and only if

$$\frac{2acdrx^*y^*}{(a+y^{*2})^2(d+x^*)^2} + \frac{(b+1)(2k-rx^*)}{k} > 0,$$

and

$$b + \frac{2acdrx^*y^*}{(a+y^{*2})^2(d+x^*)^2} - \frac{brx^*}{k} > 1.$$

Keeping in view the phase-plane analysis of positive fixed point (x^*, y^*) of system (1.2), we choose $a = 1.95$, $c = 1.1$, $d = 35$, $k = 255$ and $b = 0.85$ in ry^*-plane (cf. Fig. 5). Moreover, for $a = 5.7$, $c = 1.2$, $d = 25.5$, $r = 36.5$ and $b = 0.8$ the phase-plane analysis in ky^*-plane is depicted in Fig. 6. Finally, in ay^*-plane the phase-plane analysis of positive fixed point is depicted in Fig. 7. Taking into account Figs. 5, 6 and 7, the following results are presented.

-
- Since positive steady-state (x^*, y^*) of system (1.2) does not exist in closed form, and steady plant quality index y^* satisfies $0 < y^* < 1$, therefore it is taken as parameter.
- On the other hand, steady-state moth population x^* satisfies $0 < x^* < \frac{k}{r}\exp\left(\frac{r}{a} - 1\right)$. Consequently, upper bound for x^* is not a fixed constant, and it depends upon parametric values k, r and a.
- Therefore, it is not appropriate to consider x^* as parameter. Thus, in phase plane analysis the parameters k, r and a are used versus y^*.

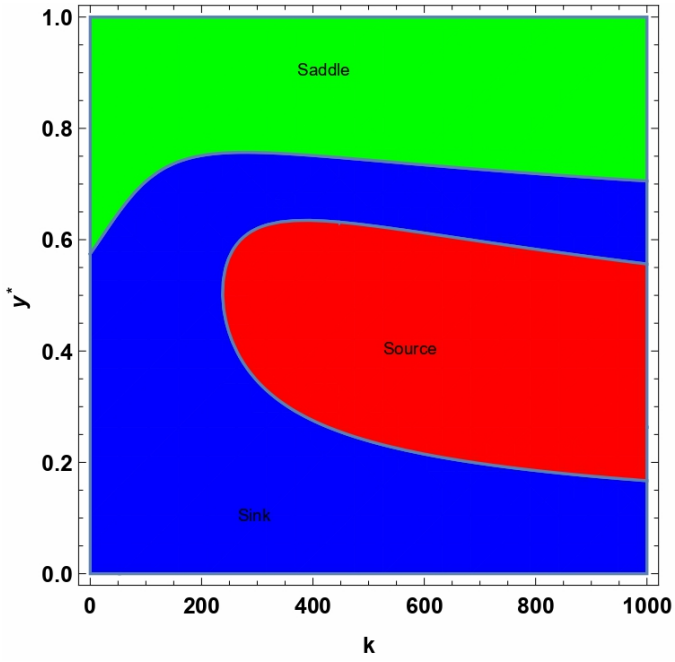

FIGURE 6. Classification of (x^*, y^*) with $a = 5.7$, $c = 1.2$, $d = 25.5$, $r = 36.5$ and $b = 0.8$ in ky^*-plane.

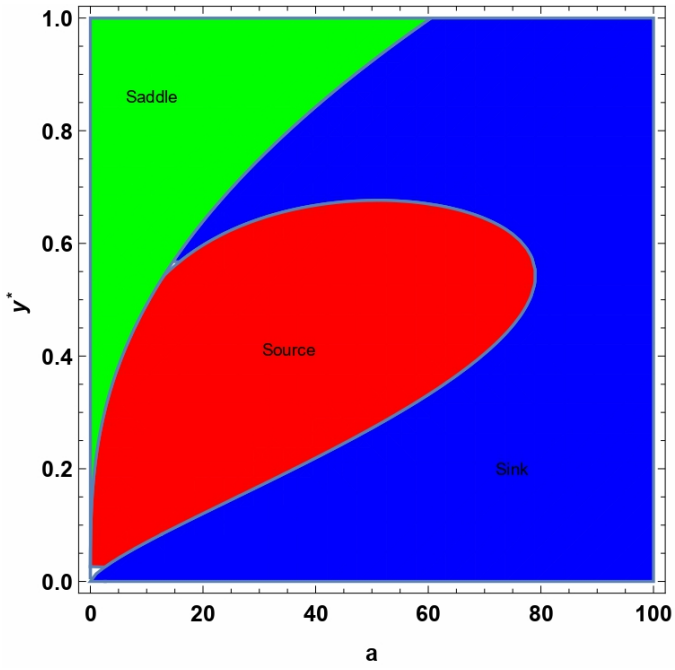

FIGURE 7. Classification of (x^*, y^*) with $k = 265$, $c = 1.32$, $d = 2.1$, $r = 176$ and $b = 0.9$ in ay^*-plane.

- In Fig. 6 as the intraspecific competition increases with very little food, the budmoth population collapses to sink.

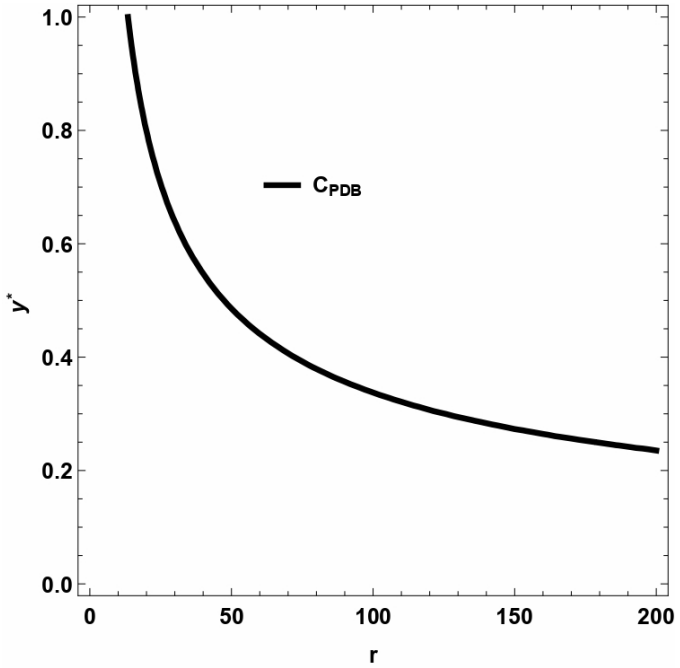

FIGURE 8. Curve C_{PDB} for $a = 5.3$, $b = 0.3$, $c = 0.25$, $d = 15$ and $k = 35$.

- In Fig. 7, it is easy to see that at the higher value of leaf content, one can expect a homoclinic orbit which may lead to fluctuations in budmoth population. Moreover, there is a source for an intermediate value of k due to less half saturation constant of moth grazing rate.

3. **Period-doubling bifurcation**

In this section, we apply bifurcation theory of normal forms and center manifold theorem for emergence of period-doubling bifurcation around interior equilibrium of system (1.2). Since positive fixed point (x^*, y^*) of system (1.2) is independent of the parameter r, therefore it is appropriate to take r as bifurcation parameter. For this, first we assume that

$$r \equiv r_0 = \frac{2(1+b)}{\frac{(1+b)x^*}{k} - \frac{2acdx^*y^*}{(a+y^{*2})^2(d+x^*)^2}}.$$

Furthermore, we define the following curve for existence of period-doubling bifurcation:

$$C_{PDB} := \left\{ (a,b,c,d,k,r) \in \mathbb{R}^6_+ : r \equiv r_0 = \frac{2(1+b)}{\frac{(1+b)x^*}{k} - \frac{2acdx^*y^*}{(a+y^{*2})^2(d+x^*)^2}} \right\}.$$

The existence of curve C_{PDB} can be verified by choosing $a = 5.3$, $b = 0.3$, $c = 0.25$, $d = 15$ and $k = 35$, then C_{PDB} is depicted in Fig. 8 in ry^*-plane. Assume that

$(a, b, c, d, k, r) \in C_{PDB}$, and writing system (1.2) in the following equivalent map:

$$\begin{pmatrix} u \\ v \end{pmatrix} \to \begin{pmatrix} u \exp\left((r_0+\bar{r})\,\left(\frac{v^2}{a+v^2}\right) - \frac{r_0+\bar{r}}{k}\,u\right) \\ 1-b+bv-\frac{cu}{d+u} \end{pmatrix}, \tag{3.1}$$

where $\bar{r}$ is very small perturbation in r_0. Furthermore, keeping in view the translations $p = u - x^*$ and $q = v - y^*$, then map (3.1) is converted into the following map with fixed point at origin:

$$\begin{pmatrix} p \\ q \end{pmatrix} \to \begin{pmatrix} \frac{k-r_0x^*}{k} & \frac{2ar_0x^*y^*}{(a+y^{*2})^2} \\ -\frac{cd}{(c+x^*)^2} & b \end{pmatrix} \begin{pmatrix} p \\ q \end{pmatrix} + \begin{pmatrix} \phi(p,q,\bar{r}) \\ \psi(p,q) \end{pmatrix}, \tag{3.2}$$

where

$$\phi(p,q,\bar{r}) = m_{13}p^2 + m_{14}pq + m_{15}q^2 + m_{16}p^3 + m_{17}p^2q + m_{18}pq^2 + m_{19}q^3 + m_1p\bar{r} + m_2q\bar{r} + m_3\bar{r}p^2 + m_4\bar{r}q^2 + m_5\bar{r}pq + O\left((|p|+|q|+|\bar{r}|)^4\right),$$

$$\psi(p,q) = m_{23}p^2 + m_{24}p^3 + O\left((|p|+|q|)^4\right),$$

$$m_{13} = -\frac{r_0(2k-r_0x^*)}{2k^2},\ m_{14} = \frac{2ar_0y^*(k-r_0x^*)}{k\left(a+y^{*2}\right)^2},\ m_{15} = \frac{ar_0x^*\left(a^2+2ay^{*2}(r_0-1)-3y^{*4}\right)}{\left(a+y^{*2}\right)^4},$$

$$m_{16} = \frac{r_0^2(3k-r_0x^*)}{6k^3},\ m_{17} = \frac{ar_0^2y^*(r_0x^*-2k)}{k^2\left(a+y^{*2}\right)^2},$$

$$m_{18} = \frac{ar_0\left(a^2+2ay^{*2}(r_0-1)-3y^{*4}\right)(k-r_0x^*)}{k\left(a+y^{*2}\right)^4},$$

$$m_{19} = \frac{2ar_0x^*y^*\left(3a^3(r_0-2)+2a^2((r_0-3)r_0-3)y^{*2}+3a(2-3r_0)y^{*4}+6y^{*6}\right)}{3\left(a+y^{*2}\right)^6},$$

$$m_1 = \frac{ax^*(r_0x^*-2k)+y^{*2}\left(k^2-kx^*(r_0+2)+r_0x^{*2}\right)}{k^2\left(a+y^{*2}\right)},$$

$$m_2 = \frac{2ax^*y^*\left(a(k-r_0x^*)+y^{*2}(kr_0+k-r_0x^*)\right)}{k\left(a+y^{*2}\right)^3},$$

$$m_3 = \frac{y^{*2}\left(-2k^2(r_0+1)+kr_0(r_0+4)x^*-r_0^2x^{*2}\right)-a\left(2k^2-4kr_0x^*+r_0^2x^{*2}\right)}{2k^3\left(a+y^{*2}\right)},$$

$$m_4 = \frac{ax^*\left(a^2+2a(2r_0-1)y^{*2}-3y^{*4}\right)}{\left(a+y^{*2}\right)^4},$$

$$m_5 = \frac{2ay^*\left(a\left(k^2-3kr_0x^*+r_0^2x^{*2}\right)+y^{*2}\left(k^2(r_0+1)-kr_0(r_0+3)x^*+r_0^2x^{*2}\right)\right)}{k^2\left(a+y^{*2}\right)^3},$$

$$m_{23} = \frac{cd}{(c+x^*)^3},\ m_{24} = -\frac{cd}{(c+x^*)^4}.$$

Suppose that $(a,b,c,d,k,r) \in C_{PDB}$, then eigenvalues of variational matrix $\begin{pmatrix} \frac{k-r_0x^*}{k} & \frac{2ar_0x^*y^*}{(a+y^{*2})^2} \\ -\frac{cd}{(c+x^*)^2} & b \end{pmatrix}$ are given by $\mu_1 = -1$ and

$$\mu_2 := \frac{a^2b(b+1)(d+x^*)^2 + 2ay^*\left(b(b+1)y^*(d+x^*)^2 - (b+2)cdk\right) + b(b+1)y^{*4}(d+x^*)^2}{a^2(b+1)(d+x^*)^2 + 2ay^*\left((b+1)y^*(d+x^*)^2 - cdk\right) + (b+1)y^{*4}(d+x^*)^2}.$$

Furthermore, assume that $|\mu_2| \neq 1$ and taking into account the following similarity transformation:

$$\begin{pmatrix} p \\ q \end{pmatrix} = T \begin{pmatrix} x \\ y \end{pmatrix}, \tag{3.3}$$

where

$$T = \begin{pmatrix} m_{12} & m_{12} \\ -1 - m_{11} & \mu_2 - m_{11} \end{pmatrix},$$

where

$$m_{11} = \frac{k - r_0x^*}{k}$$

and

$$m_{12} = \frac{2ar_0x^*y^*}{(a + y^{*2})^2}.$$

From (3.2) and (3.3), we obtain

$$\begin{pmatrix} x \\ y \end{pmatrix} \to \begin{pmatrix} -1 & 0 \\ 0 & \mu_2 \end{pmatrix} \begin{pmatrix} x \\ y \end{pmatrix} + \begin{pmatrix} \phi_1(x,y,\bar{r}) \\ \psi_1(x,y,\bar{r}) \end{pmatrix}, \tag{3.4}$$

where

$$\begin{aligned}
\phi_1(x,y,\bar{r}) = &-\left(\frac{m_{13}m_{11} + m_{23}m_{12} - m_{13}\mu_2}{m_{12}(\mu_2+1)}\right)p^2 + \left(\frac{(\mu_2 - m_{11})m_{14}}{m_{12}(\mu_2+1)}\right)pq + \left(\frac{(\mu_2 - m_{11})m_{15}}{m_{12}(\mu_2+1)}\right)q^2 \\
&-\left(\frac{m_{11}m_{16} + m_{12}m_{24} - m_{16}\mu_2}{m_{12}(\mu_2+1)}\right)p^3 + \left(\frac{(\mu_2 - m_{11})m_{17}}{m_{12}(\mu_2+1)}\right)p^2q + \left(\frac{(\mu_2 - m_{11})m_{18}}{m_{12}(\mu_2+1)}\right)pq^2 \\
&+\left(\frac{(\mu_2 - m_{11})m_{19}}{m_{12}(\mu_2+1)}\right)q^3 + \left(\frac{(\mu_2 - m_{11})m_1}{m_{12}(\mu_2+1)}\right)p\bar{r} + \left(\frac{(\mu_2 - m_{11})m_2}{m_{12}(\mu_2+1)}\right)q\bar{r} \\
&+\left(\frac{(\mu_2 - m_{11})m_3}{m_{12}(\mu_2+1)}\right)\bar{r}p^2 + \left(\frac{(\mu_2 - m_{11})m_4}{m_{12}(\mu_2+1)}\right)\bar{r}q^2 + \left(\frac{(\mu_2 - m_{11})m_5}{m_{12}(\mu_2+1)}\right)\bar{r}pq \\
&+O\left((|x|+|y|+|\bar{r}|)^4\right),
\end{aligned}$$

$$\psi_1(x,y,\bar{r}) = \left(\frac{(1+m_{11})\,m_{13}}{m_{12}\,(\mu_2+1)} + \frac{m_{23}}{\mu_2+1}\right)p^2 + \left(\frac{(1+m_{11})\,m_{14}}{m_{12}\,(\mu_2+1)}\right)pq + \left(\frac{(1+m_{11})\,m_{15}}{m_{12}\,(\mu_2+1)}\right)q^2$$
$$+ \left(\frac{(1+m_{11})\,m_{16}}{m_{12}\,(\mu_2+1)} + \frac{m_{24}}{\mu_2+1}\right)p^3 + \left(\frac{(1+m_{11})\,m_{17}}{m_{12}\,(\mu_2+1)}\right)p^2q + \left(\frac{(1+m_{11})\,m_{18}}{m_{12}\,(\mu_2+1)}\right)pq^2$$
$$+ \left(\frac{(1+m_{11})\,m_{19}}{m_{12}\,(\mu_2+1)}\right)q^3 + \left(\frac{(1+m_{11})\,m_1}{m_{12}\,(\mu_2+1)}\right)p\bar{r} + \left(\frac{(1+m_{11})\,m_2}{m_{12}\,(\mu_2+1)}\right)q\bar{r}$$
$$+ \left(\frac{(1+m_{11})\,m_3}{m_{12}\,(\mu_2+1)}\right)\bar{r}p^2 + \left(\frac{(1+m_{11})\,m_4}{m_{12}\,(\mu_2+1)}\right)\bar{r}q^2 + \left(\frac{(1+m_{11})\,m_5}{m_{12}\,(\mu_2+1)}\right)\bar{r}pq$$
$$+ O\left((|x|+|y|+|\bar{r}|)^4\right),$$
$$p = m_{12}(x+y) \text{ and } q = -(1+m_{11})x + (\mu_2 - m_{11})y.$$

Due to center manifold theory [21], stability analysis of equilibrium $(x,y) = (0,0)$ near $\bar{r} = 0$ can be discussed by investigating a one–parameter family of reduced equations on a center manifold $W^C(0,0,0)$, which can be described as follows:

$$W^C(0,0,0) = \left\{(x,y,\bar{r}) \in \mathbb{R}^3 : y = l_1x^2 + l_2x\bar{r} + l_3\bar{r}^2 + O\left((|x|+|\bar{r}|)^3\right)\right\},$$

where

$$l_1 = \frac{m_{11}^2m_{14} - m_{11}m_{12}m_{13} - m_{12}^2m_{23} + 2m_{11}m_{14} - m_{12}m_{13} + m_{14}}{\mu_2^2 - 1}$$
$$+ \frac{m_{15}\,(1+m_{11})^3}{m_{12}\,(1-\mu_2^2)},$$
$$l_2 = \frac{(1+m_{11})\,(m_1m_{12} - m_2m_{11} - m_2)}{m_{12}\,(1-\mu_2^2)},\ l_3 = 0.$$

On the other hand, the map restricted to center manifold is described as follows:

$$\Omega : x \to -x + d_1x^2 + d_2x\bar{r} + d_3x^2\bar{r} + d_4x\bar{r}^2 + d_5x^3 + O\left((|x|+|\bar{r}|)^4\right),$$

where

$$d_1 = \left(\frac{(\mu_2 - m_{11})\,m_{13}}{m_{12}\,(\mu_2+1)} - \frac{m_{23}}{\mu_2+1}\right)m_{12}^2 - \frac{(\mu_2 - m_{11})\,m_{14}\,(1+m_{11})}{\mu_2+1}$$
$$+ \frac{(\mu_2 - m_{11})\,m_{15}\,(1+m_{11})^2}{m_{12}\,(\mu_2+1)},$$
$$d_2 = \frac{(\mu_2 - m_{11})\,m_1}{\mu_2+1} - \frac{(\mu_2 - m_{11})\,m_2\,(1+m_{11})}{m_{12}\,(\mu_2+1)},$$
$$d_3 = \frac{(\mu_2 - m_{11})\,m_{12}m_3}{\mu_2+1} - \frac{(\mu_2 - m_{11})\,m_5\,(1+m_{11})}{\mu_2+1} + \frac{(\mu_2 - m_{11})\,m_1l_1}{\mu_2+1}$$
$$+ \frac{(\mu_2 - m_{11})\,m_4\,(1+m_{11})^2}{m_{12}\,(\mu_2+1)} + \frac{(\mu_2 - m_{11})^2\,m_2l_1}{m_{12}\,(\mu_2+1)} + 2\left(\frac{(\mu_2 - m_{11})\,m_{13}}{m_{12}\,(\mu_2+1)} - \frac{m_{23}}{\mu_2+1}\right)m_{12}^2l_2$$
$$+ \frac{(\mu_2 - m_{11})^2\,m_{14}l_2}{\mu_2+1} - \frac{(\mu_2 - m_{11})\,m_{14}l_2\,(1+m_{11})}{\mu_2+1} - 2\,\frac{(\mu_2 - m_{11})^2\,m_{15}\,(1+m_{11})\,l_2}{m_{12}\,(\mu_2+1)},$$
$$d_4 = \frac{(\mu_2 - m_{11})\,l_2\,(m_1m_{12} - m_2m_{11} + m_2\mu_2)}{m_{12}\,(\mu_2+1)},$$

and

$$\begin{aligned} d_5 = & \left(\frac{(\mu_2 - m_{11})\, m_{16}}{m_{12}\,(\mu_2+1)} - \frac{m_{24}}{\mu_2+1} \right) m_{12}^3 - \frac{(\mu_2 - m_{11})\, m_{12} m_{17}\,(1+m_{11})}{\mu_2+1} \\ & + 2\left(\frac{(\mu_2 - m_{11})\, m_{13}}{m_{12}\,(\mu_2+1)} - \frac{m_{23}}{\mu_2+1} \right) m_{12}^2 l_1 + \frac{(\mu_2 - m_{11})\, m_{18}\,(1+m_{11})^2}{\mu_2+1} \\ & - \frac{(\mu_2 - m_{11})\, m_{14} l_1\,(1+m_{11})}{\mu_2+1} - \frac{(\mu_2 - m_{11})\, m_{19}\,(1+m_{11})^3}{m_{12}\,(\mu_2+1)} \\ & + \frac{(\mu_2 - m_{11})^2\, m_{14} l_1}{\mu_2+1} - \frac{2\,(\mu_2 - m_{11})^2\, m_{15}\,(1+m_{11})\, l_1}{m_{12}\,(\mu_2+1)}. \end{aligned}$$

On the other hand, two nonzero numbers k_1 and k_2 are computed as follows:

$$\begin{aligned} k_1 = & \left(\frac{\partial^2 \phi_1}{\partial x \partial \bar{r}} + \frac{1}{2}\frac{\partial \Omega}{\partial \bar{r}}\frac{\partial^2 \Omega}{\partial x^2} \right)_{(0,0)} \\ = & \frac{(\mu_2 - m_{11})\, m_1}{\mu_2+1} - \frac{(\mu_2 - m_{11})\, m_2\,(1+m_{11})}{m_{12}\,(\mu_2+1)}, \end{aligned}$$

and

$$k_2 = \left(\frac{1}{6}\frac{\partial^3 \Omega}{\partial x^3} + \left(\frac{1}{2}\frac{\partial^2 \Omega}{\partial x^2} \right)^2 \right)_{(0,0)} = d_1^2 + d_5.$$

Keeping in view above computation, the following Lemma gives the parametric conditions for existence and direction of flip bifurcation for system (1.2) at its positive fixed point.

Theorem 3.1. *Suppose that $k_1 \neq 0$ and $k_2 \neq 0$, then system (1.2) undergoes period-doubling bifurcation at its positive steady-state (x^*, y^*) when parameter r varies in small neighborhood of r_0. Furthermore, if $k_2 > 0$, then the period-two orbits that bifurcate from (x^*, y^*) are stable, and if $k_2 < 0$, then these orbits are unstable.*

4. **Neimark-Sacker bifurcation**

In this section, we discuss that system (1.2) undergoes Neimark-Sacker bifurcation around its positive equilibrium (x^*, y^*). For this, r is taken as bifurcation parameter. For emergence of Neimark-Sacker bifurcation around positive equilibrium (x^*, y^*) of system (1.2), the roots of (2.6) must be complex conjugate with unit modulus. Therefore, necessary conditions for emergence of Neimark-Sacker about positive fixed point of system (1.2) are described by the following curve:

$$C_{NB} = \left\{ (a,b,c,d,k,r) \in \mathbb{R}_+^6 : r \equiv r_1 = \frac{1-b}{\frac{2acdx^*y^*}{(a+y^{*2})^2(d+x^*)^2} - \frac{bx^*}{k}},\ \left| b + \frac{k - r_1 x^*}{k} \right| < 2 \right\}.$$

It is easy to see that C_{NB} is nonempty because for $a = 8.5$, $b = 0.25$, $c = 1.25$, $d = 10$ and $k = 165$, this curve C_{NB} is depicted in Fig. 9 in ry^*-plane. Assuming that $\tilde{r}$

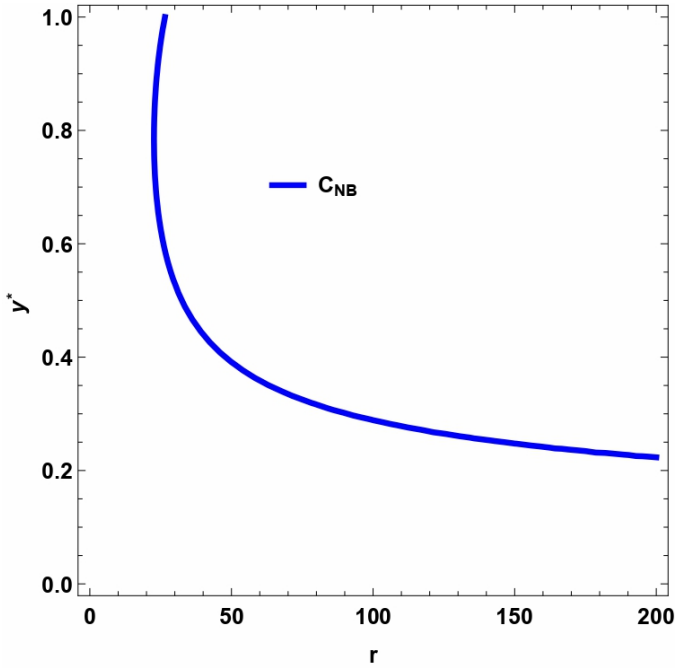

FIGURE 9. Existence of curve C_{NB} for $a = 8.5$, $b = 0.25$, $c = 1.25$, $d = 10$ and $k = 165$ in ry^*-plane.

be a small perturbation in $r \equiv r_1$, then system (1.2) is described by the following 2-dimensional map:

$$\begin{pmatrix} U \\ V \end{pmatrix} \to \begin{pmatrix} U \exp\left((r_1+\tilde{r})\left(\frac{V^2}{a+V^2}\right) - \frac{r_1+\tilde{r}}{k}U\right) \\ 1-b+bV-\frac{cU}{d+U} \end{pmatrix}. \tag{4.1}$$

Suppose that (x^*, y^*) be unique positive fixed point of the map (4.1), then we consider the translations $u = U - x^*$ and $v = V - y^*$ for shifting the fixed point of resulting map at origin. Consequently, these translations yield the following map with fixed point at origin:

$$\begin{pmatrix} u \\ v \end{pmatrix} \to \begin{pmatrix} a_{11} & a_{12} \\ a_{21} & a_{22} \end{pmatrix} \begin{pmatrix} u \\ v \end{pmatrix} + \begin{pmatrix} f(u,v) \\ g(u,v) \end{pmatrix}, \tag{4.2}$$

where

$$f(u,v) = a_{13}u^2 + a_{14}uv + a_{15}v^2 + a_{16}u^3 + a_{17}u^2v + a_{18}uv^2 + a_{19}v^3 + O\left((|u|+|v|)^4\right),$$

$$g(u,v) = a_{23}u^2 + a_{24}u^3 + O\left((|u|+|v|)^4\right),$$

$$\begin{pmatrix} a_{11} & a_{12} \\ a_{21} & a_{22} \end{pmatrix} = \begin{pmatrix} \frac{k-(r_1+\tilde{r})x^*}{k} & \frac{2a(r_1+\tilde{r})x^*}{(a+y^{*2})^2} \\ -\frac{cd}{(c+x^*)^2} & b \end{pmatrix}, \; a_{13} = -\frac{R(2k-Rx^*)}{2k^2},$$

$$a_{14} = \frac{2aRy^*(k-Rx^*)}{k\left(a+y^{*2}\right)^2}, \; a_{15} = \frac{aRx^*\left(a^2+2a(R-1)y^{*2}-3y^{*4}\right)}{\left(a+y^{*2}\right)^4},$$

$$a_{16}=\frac{R^2(3k-Rx^*)}{6k^3},\ a_{17}=\frac{aR^2y^*(Rx^*-2k)}{k^2\left(a+y^{*2}\right)^2},$$
$$a_{18}=\frac{aR\left(a^2+2a(R-1)y^{*2}-3y^{*4}\right)(k-Rx^*)}{k\left(a+y^{*2}\right)^4},$$
$$a_{19}=\frac{2aRx^*y^*\left(3a^3(R-2)+2a^2((R-3)R-3)y^{*2}+3a(2-3R)y^{*4}+6y^{*6}\right)}{3\left(a+y^{*2}\right)^6},$$
$$a_{23}=\frac{cd}{(c+x^*)^3},\ a_{24}=-\frac{cd}{(c+x^*)^4},\ R=r_1+\tilde{r}.$$

Now, characteristic polynomial of map (4.2) at its fixed point $(0,0)$ is given by

$$P(\tau)=\tau^2-A(\tilde{r})\tau+B(\tilde{r}), \tag{4.3}$$

where

$$A(\tilde{r}):=b+\frac{k-(r_1+\tilde{r})x^*}{k},$$

and

$$B(\tilde{r}):=b+\frac{2acd(r_1+\tilde{r})x^*y^*}{\left(a+y^{*2}\right)^2(d+x^*)^2}-\frac{b(r_1+\tilde{r})x^*}{k}.$$

Moreover, complex conjugate roots of (4.3) are given by

$$\tau_1=\frac{A(\tilde{r})+\iota\sqrt{4B(\tilde{r})-A^2(\tilde{r})}}{2},$$

and

$$\tau_2=\frac{A(\tilde{r})-\iota\sqrt{4B(\tilde{r})-A^2(\tilde{r})}}{2}.$$

Then, simple computation yields that $|\tau_1|=|\tau_2|=\sqrt{B(\tilde{r})}$. Next, in order to verify nondegeneracy conditions, first we see that:

$$\left(\frac{d|\tau_{1,2}|}{d\tilde{r}}\right)_{\tilde{r}=0}=\frac{acdx^*y^*}{\left(a+y^{*2}\right)^2(d+x^*)^2}-\frac{bx^*}{2k}\neq 0.$$

Secondly, keeping in view non-resonance, at $\tilde{r}=0$ it is required that $\tau_{1,2}^n\neq 1$ for $n=1,2,3,4$, which is equivalent to $A(0)\neq -2,-1,0,2$. Assume that $(a,b,c,d,k,r)\in C_{NB}$, then it follows that $|A(0)|<2$. Moreover, we have

$$A(0)=b+\frac{k-r_1x^*}{k}.$$

Therefore, conditions for non-resonance are satisfied if the following holds true:

$$b+\frac{k-r_1x^*}{k}\neq 0,-1.$$

Furthermore, in order to compute the first Lyapunov exponent, we want to transform Jacobian matrix of (4.2) into canonical form. For this, the following transformation is considered:

$$\begin{pmatrix} u \\ v \end{pmatrix}=\begin{pmatrix} a_{12} & 0 \\ \alpha-a_{11} & -\beta \end{pmatrix}\begin{pmatrix} w \\ z \end{pmatrix}, \tag{4.4}$$

where

$$\alpha := \frac{A(0)}{2} \text{ and } \beta := \frac{\sqrt{4B(0) - A^2(0)}}{2}.$$

Consequently, from (4.2) and (4.4), it follows that

$$\begin{pmatrix} w \\ z \end{pmatrix} \to \begin{pmatrix} \alpha & -\beta \\ \beta & \alpha \end{pmatrix} \begin{pmatrix} w \\ z \end{pmatrix} + \begin{pmatrix} M(w,z) \\ N(w,z) \end{pmatrix}, \tag{4.5}$$

where

$$M(w,z) := \frac{1}{a_{12}} f\Big(a_{12}w, (\alpha - a_{11})w - \beta z\Big),$$

and

$$N(w,z) := -\frac{a_{11}-\alpha}{a_{12}\beta} f\Big(a_{12}w, (\alpha - a_{11})w - \beta z\Big) - \frac{1}{\beta} g\Big(a_{12}w, (\alpha - a_{11})w - \beta z\Big).$$

Keeping in view the normal forms theory related to bifurcation analysis [22, 23, 24, 25, 26], at $(w, z, \tilde{r}) = (0, 0, 0)$ the first Lyapunov exponent is computed as follows:

$$L = -Re\left(\frac{(1-2\tau_1)\tau_2^2}{1-\tau_1}\tau_{20}\tau_{11}\right) - \frac{1}{2}|\tau_{11}|^2 - |\tau_{02}|^2 + Re(\tau_2\tau_{21}),$$

where

$$\tau_{20} = \frac{1}{8}\Big[M_{ww} - M_{zz} + 2N_{wz} + i(N_{ww} - N_{zz} - 2M_{wz})\Big],$$

$$\tau_{11} = \frac{1}{4}\Big[M_{ww} + M_{zz} + i(N_{ww} + N_{zz})\Big],$$

$$\tau_{02} = \frac{1}{8}\Big[M_{ww} - M_{zz} - 2N_{wz} + i(N_{ww} - N_{zz} + 2M_{wz})\Big],$$

and

$$\tau_{21} = \frac{1}{16}\Big[M_{www} + M_{wzz} + N_{wwz} + N_{zzz} + i(N_{www} + N_{wzz} - M_{wwz} - M_{zzz})\Big].$$

Then, due to above calculation, one has the following Theorem:

Theorem 4.1. *Assume that* $(a, b, c, d, k, r) \in C_{NB}$, $\frac{acdx^*y^*}{(a+y^{*2})^2(d+x^*)^2} - \frac{bx^*}{2k} \neq 0$, $b + \frac{k-r_1x^*}{k} \neq 0, -1$ *and* $L \neq 0$, *then unique positive equilibrium point* (x^*, y^*) *of system* (1.2) *undergoes Neimark-Sacker bifurcation when the bifurcation parameter* r *varies in a small neighborhood of* $r_1 = \frac{1-b}{\frac{2acdx^*y^*}{(a+y^{*2})^2(d+x^*)^2} - \frac{bx^*}{k}}$. *Moreover, if* $L > 0$, *then a stable invariant closed curve bifurcates from the equilibrium point for* $r > r_1$, *and if* $L < 0$, *then an unstable invariant closed curve bifurcates from the equilibrium point for* $r < r_1$.

5. **Chaos control**

Comparatively small perturbations are added to control chaotic behavior of a given system and in a return unstable orbits become stable one. Consequently, the implementation of chaos control strategies makes chaotic orbits more predictable and stable. The successful chaos control method plays important role for stabilization of perturbed system and avoids from fluctuating and unpredictable situations. The perturbation added to corresponding controlled system must be negligible as compare to chaotic or bifurcating system to avoid from major modification of natural dynamics of original system.

This section is dedicated for implementation of chaos control methods to system (1.2). For this, three chaos control methods are implemented to system (1.2). Implementation of chaos control methods for discrete-time systems is topic of great interest. Recently, many discrete-time systems have been discussed for implementation of strategies related to chaos and bifurcations control [27, 28, 29, 30, 31, 32, 33, 34, 35, 36, 37, 38, 39, 40, 41].

First, we consider Ott-Grebogi-Yorke (OGY) method (see [42]). An application of OGY feedback control method to system (1.2) yields the following control system:

$$\begin{aligned} x_{n+1} &= x_n \exp\left(\Pi\left(\frac{y_n^2}{a+y_n^2}\right) - \frac{\Pi}{k}\, x_n\right), \\ y_{n+1} &= (1-b) + by_n - \frac{cx_n}{d+x_n}, \end{aligned} \tag{5.1}$$

where

$$\Pi := r - c_1(x_n - x^*) - c_2(y_n - y^*),$$

c_1 and c_2 are control parameters, and (x^*, y^*) is interior equilibrium point of system (1.2). Furthermore, biological relevance of OGY method and its control parameters is given as follows:

-
- In the case of OGY, the chaos control is applied by including a harvesting term equal to the difference between the current value and the equilibrium value quantity, to the larch bud moth growth rate. Essentially this feedback tries to bring the system back close to an equilibrium position.
- c_1 represents refuge rate of budmoth population density $x_n - x^*$ at time n.
- Assume that some sort of insecticide spray is provided to the plant quality index $y_n - y^*$, which may affect the growth rate of budmoth up to a certain level, say c_2.

In order to see the controllability of system (5.1), first we compute controllability matrix C for this system as follows:

$$C = \left[B_{(x^*,y^*,r_2)} : A_{(x^*,y^*,r_2)}B_{(x^*,y^*,r_2)}\right],$$

where $A_{(x^*,y^*,r_2)}$ is Jacobian matrix of system (1.2) computed at (x^*, y^*, r_2), (x^*, y^*) is positive fixed point of (1.2), r_2 is critical value of bifurcation parameter r lies in bifurcating or chaotic interval, that is, $r_2 \geq r_0$ or $r_2 \geq r_1$, and $B_{(x^*,y^*,r_2)}$ is given as follows:

$$B_{(x^*,y^*,r_2)} = \begin{pmatrix} \frac{\partial f(x^*,y^*,r_2)}{\partial r} \\ \frac{\partial g(x^*,y^*,r_2)}{\partial r} \end{pmatrix},$$

where

$$f(x, y, r) = x \exp\left(r\left(\frac{y^2}{a+y^2}\right) - \frac{r}{k}x\right),$$

and

$$g(x, y, r) = (1-b) + by - \frac{cx}{d+x}.$$

Keeping in view the fact that (x^*, y^*) satisfies $\frac{y^{*2}}{a+y^{*2}} - \frac{x^*}{k} = 0$, one has $\frac{\partial f(x^*,y^*,r_2)}{\partial r} = x^*\left(\frac{y^{*2}}{a+y^{*2}} - \frac{x^*}{k}\right) = 0$ and $\frac{\partial g(x^*,y^*,r_2)}{\partial r} = 0$. Consequently, C is a null matrix of order 2×2. Hence, rank of controllability matrix C is zero. Hence, OGY method is not applicable for controlling chaotic behavior of system (1.2) at (x^*, y^*, r_2).

Secondly, we apply hybrid control method [43] to system (1.2) to get the following control system:

$$\begin{aligned} x_{n+1} &= \alpha\left(x_n \exp\left(r\left(\frac{y_n^2}{a+y_n^2}\right) - \frac{r}{k}x_n\right)\right) + (1-\alpha)x_n, \\ y_{n+1} &= \alpha\left((1-b) + by_n - \frac{cx_n}{d+x_n}\right) + (1-\alpha)y_n, \end{aligned} \tag{5.2}$$

where $0 < \alpha < 1$ is control parameter for hybrid control method, which is based on parameter perturbation and state feedback control. The biological relevance of hybrid control method is stated as follows:

-
- From control system (5.2), it is easy to observe that the growth rate is increased by α and the $1-\alpha$ harvesting term is introduced as a correction to the equations.
- Consequently, the leaf available for the budmoth is reduced by $\alpha(b-1)+1$. By forcing the food source to be less, the budmoths are not allowed to grow. This is also evident in Fig. 10.

Again controllability of system (5.2) depends upon stability of this system at its positive fixed point. To see this stability behavior, the Jacobian matrix $J_H(x^*, y^*)$ of system (5.2) at its unique positive fixed point (x^*, y^*) is given as follows:

$$J_H(x^*, y^*) = \begin{pmatrix} 1 - \frac{\alpha r x^*}{k} & \frac{2a\alpha r x^* y^*}{(a+y^{*2})^2} \\ -\frac{\alpha cd}{(c+x^*)^2} & 1-\alpha(1-b) \end{pmatrix}.$$

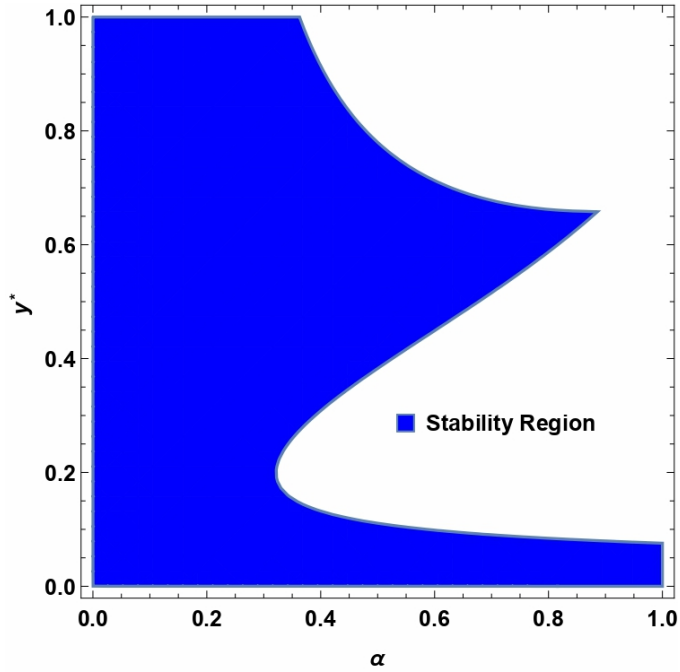

FIGURE 10. Controllable region of (5.2) for $a = 0.75$, $b = 0.15$, $c = 3.2$, $d = 6.3$, $r = 10$ and $k = 165$ in αy^*-plane.

In addition, the characteristic polynomial for $J_H(x^*, y^*)$ is computed as follows:

(5.3)
$$F(\mu) = \mu^2 - \left(2 + \alpha\left(b - \frac{rx^*}{k} - 1\right)\right)\mu + (1 - \alpha + \alpha b)\left(1 - \frac{\alpha r x^*}{k}\right) + \frac{2a\alpha^2 cdrx^*y^*}{\left(a + y^{*2}\right)^2 (d + x^*)^2}.$$

Taking into account the controllability of system (5.2), the following Lemma is presented.

Lemma 5.1. *Positive fixed point (x^*, y^*) of system (5.2) is a sink if the following condition is satisfied:*

$$\left|2 + \alpha\left(b - \frac{rx^*}{k} - 1\right)\right| < 1 + (1 - \alpha + \alpha b)\left(1 - \frac{\alpha r x^*}{k}\right) + \frac{2a\alpha^2 cdrx^*y^*}{\left(a + y^{*2}\right)^2 (d + x^*)^2} < 2.$$

Clearly, controllability of system (5.2) depends upon the choice of parametric values of given system (1.2) and α. For $a = 0.75$, $b = 0.15$, $c = 3.2$, $d = 6.3$, $r = 10$ and $k = 165$, controllable region of (5.2) is depicted in Fig. 10 in αy^*-plane. The area of stability region varies (increases or decreases) with variation in parametric values. At the end of this section, we apply recently proposed chaos control method of exponential type to system (1.2) as follows [34]:

(5.4)
$$\begin{aligned} x_{n+1} &= \exp\left(-s_1(x_n - x^*)\right) x_n \exp\left(r\left(\frac{y_n^2}{a + y_n^2}\right) - \frac{r}{k}x_n\right), \\ y_{n+1} &= \exp\left(-s_2(y_n - y^*)\right)\left((1 - b) + by_n - \frac{cx_n}{d + x_n}\right), \end{aligned}$$

where s_1 and s_2 are control parameters, and (x^*, y^*) is interior fixed point of system (1.2).

According to [10, 15, 16], some seasonal effects may result migration of budmoth population, and a change in plant quality index. Keeping in view these studies, the biological interpretation of control system (5.4) is given as follows:

-
- The function $\exp(-s_1(x_n - x^*))$ represents exponential type density-dependent harvesting of budmoth population $x_n - x^*$.
- s_1 is harvesting rate of budmoth population $x_n - x^*$. Moreover, for $s_1 > 0$ it is an emigration rate, and for $s_1 < 0$ it is an immigration rate for this population.
- Due to climate change, $\exp(-s_2(y_n - y^*))$ denotes exponential type density-dependent harvesting of plant quality index $y_n - y^*$.
- s_2 is harvesting rate of plant quality index $y_n - y^*$. Moreover, $s_2 > 0$ will decrease, and $s_2 < 0$ will increase the plant quality index.

In order to see the effectiveness of exponential chaos control method about its positive fixed point (x^*, y^*), we have to focus on local stability of system (5.4) about (x^*, y^*). For this, the variational matrix $J_E(x^*, y^*)$ of system (5.4) is computed as follows:

$$J_E(x^*, y^*) = \begin{pmatrix} \frac{k - x^*(ks_1 + r)}{k} & \frac{2arx^*y^*}{(a + y^{*2})^2} \\ -\frac{cd}{(c + x^*)^2} & b - s_2y^* \end{pmatrix}.$$

In addition, the characteristic polynomial for $J_E(x^*, y^*)$ is computed as follows:

$$\begin{aligned} F(\nu) = \nu^2 - \left(1 + b - \frac{x^*(ks_1 + r)}{k} - s_2y^*\right)\nu + \frac{2acdrx^*y^*}{(a + y^{*2})^2(d + x^*)^2} \\ + (b - s_2y^*)\left(\frac{k - x^*(ks_1 + r)}{k}\right). \end{aligned} \tag{5.5}$$

Taking into account the controllability of system (5.4), the following Lemma is presented.

Lemma 5.2. *Positive fixed point (x^*, y^*) of system (5.4) is a sink if the following condition is satisfied:*

$$\begin{aligned} \left|\frac{k - x^*(ks_1 + r)}{k} + b - s_2y^*\right| < 1 + \frac{2acdrx^*y^*}{(a + y^{*2})^2(d + x^*)^2} \\ + (b - s_2y^*)\left(\frac{k - x^*(ks_1 + r)}{k}\right) < 2. \end{aligned}$$

For $a = 3.8$, $b = 0.45$, $c = 1.5$, $d = 1.2$, $k = 0.35$ and $r = 1.85$, controllable region of (5.4) is depicted in Fig. 11 in $y^*s_1s_2$-space.

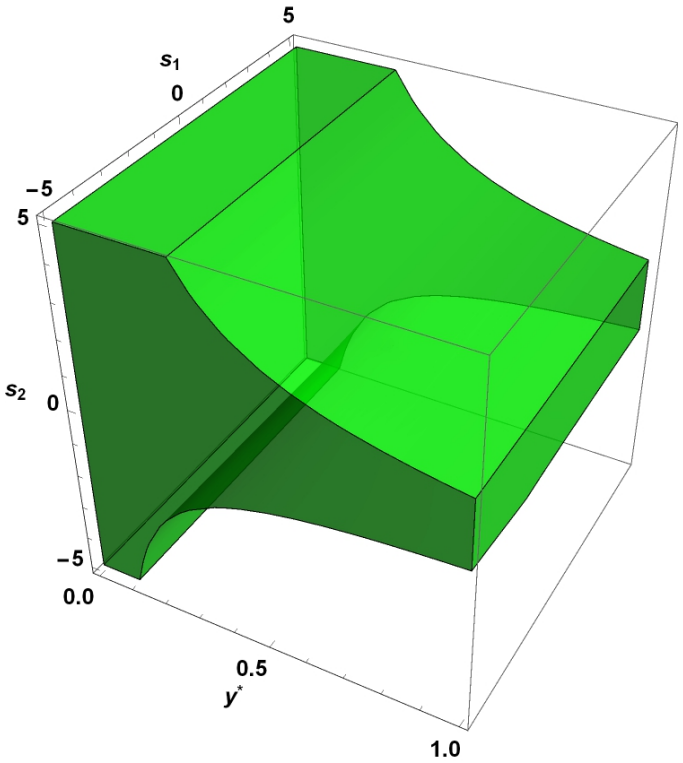

FIGURE 11. Controllable region of (5.4) for $a = 3.8$, $b = 0.45$, $c = 1.5$, $d = 1.2$, $k = 0.35$ and $r = 1.85$ in $y^* s_1 s_2$-space.

Parameter of system (1.2)	Parameter estimates	Source
r	2.5 ± 0.2	[11]
a	88.14 ± 61.75	[18]
k	500 ± 200	[11]
b	0.5 ± 0.1	[11]
c	0.7 ± 0.2	[11]
d	150 ± 150	[11]

TABLE 2. Regression–based parameter estimates for system (1.2).

6. **Numerical simulation and discussion**

For the validation of our theoretical findings with respect to observed field data, the following parametric estimations are presented, which are based on statistical analysis reported by Turchin [11] and parameter a is fitted keeping in view the data reported by Baltensweiler *et al.* [18] in Engadine (Switzerland). Case (i): Keeping in view Table 2, first we consider the best fitted values for parameters $k = 500 \in [300, 700]$, $a = 88.14 \in [26.3846, 149.889]$, $d = 150 \in [0, 300]$,

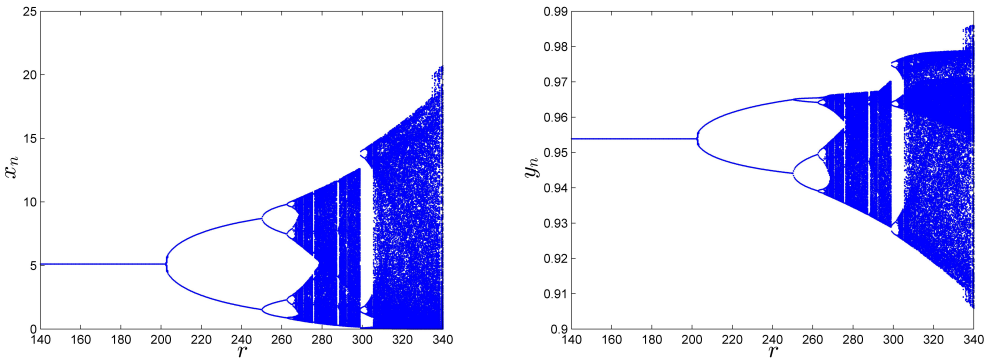

(A) Bifurcation diagram for x_n (B) Bifurcation diagram for y_n

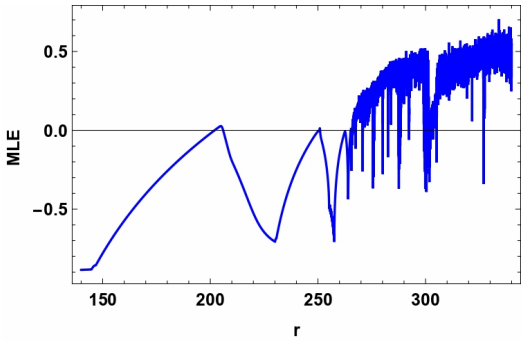

(C) Maximum Lyapunov exponents

FIGURE 12. Bifurcation diagrams and MLE for system (1.2) with $a = 88.14$, $b = 0.5$, $c = 0.7$, $d = 150$, $k = 500$, $r \in [140, 340]$ and $(x_0, y_0) = (5.1089, 0.9538)$.

$b = 0.5 \in [0.4, 0.6]$, $c = 0.7 \in [0.5, 0.9]$ and r is taken as bifurcation parameter. Then, system (1.2) undergoes period-doubling bifurcation around its interior equilibrium $(x^*, y^*) = (5.10894, 0.953887)$ when r passes through the critical value $r_0 = 201.966$. On the other hand, at $a = 88.14$, $b = 0.5$, $c = 0.7$, $d = 150$, $k = 500$ and $r = 201.966$ the multipliers of system (1.2) are $\mu_1 = -1$ and $\mu_2 = 0.43634$ with $|\mu_2| \neq 1$. Moreover, bifurcation diagrams and maximum Lyapunov exponents (MLE) of system are depicted in Fig. 12.

Next, we demonstrate validity of chaos control methods related to period-doubling bifurcation. For this, first we see the effectiveness of hybrid control method. Assume that $a = 88.14$, $b = 0.5$, $c = 0.7$, $d = 150$ and $k = 500$ are substituted in system (5.2). A variation in controllability interval is observed with variation of bifurcation parameter r in chaotic region $[201.966, 340]$. Due to this variation, it is observed that length of controllability interval can be increased by shifting the value of bifurcation parameter at the left end of chaotic region. Variation of controllability with respect to control parameter r is distributed in Fig. 13 in $r\alpha$-plane. Similarly, to see the effectiveness of third chaos control method (exponential control), we choose

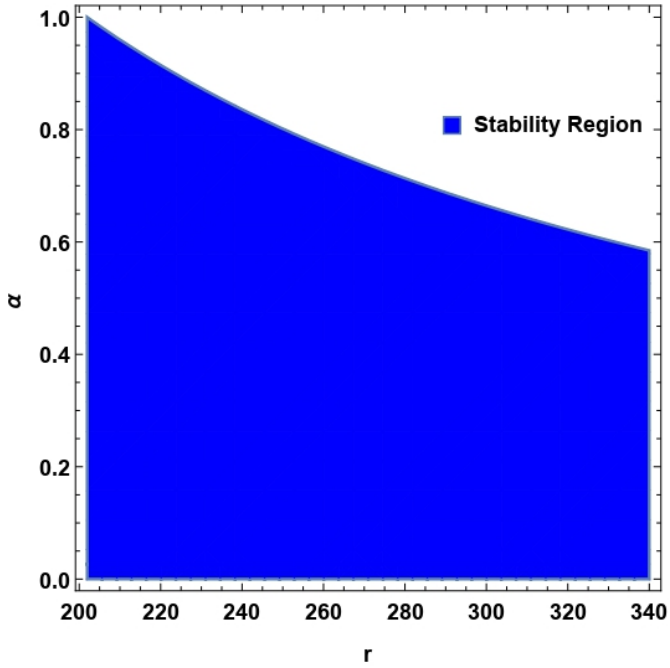

FIGURE 13. For $a = 88.14$, $b = 0.5$, $c = 0.7$, $d = 150$ and $k = 500$ controllability region of system (5.2).

$a = 88.14$, $b = 0.5$, $c = 0.7$, $d = 150$ and $k = 500$ for system (5.4). For these selected values and $r \in [201.966, 340]$, the controllability region of system (5.4) is depicted in Fig. 14 in rs_1s_2-space. Case (ii): Secondly, for demonstration of Neimark-Sacker bifurcation in system (1.2), we choose parametric values of system (1.2) as follows: $k = 350 \in [300, 700]$, $a = 50.23 \in [26.3846, 149.889]$, $d = 0.9 \in [0, 300]$, $b = 0.4 \in [0.4, 0.6]$, $c = 0.9 \in [0.5, 0.9]$ and $r \in [240, 380]$ with initial conditions $(x_0,\ y_0) = (0.7357,\ 0.325)$. Then, system (1.2) undergoes Neimark-Sacker bifurcation about fixed point $(x^*, y^*) = (0.735778, 0.325295)$ with critical value of bifurcation parameter $r_1 = 295.294$. On the other hand, at $k = 350$, $a = 50.23$, $d = 0.9$, $b = 0.4$, $c = 0.9$ and $r = 295.294$, the characteristic polynomial for variational matrix of system (1.2) is calculated as follows:

$$P(\tau) = \tau^2 - 0.779227\tau + 1.$$

Then, multipliers of variational matrix (roots of $P(\tau)$) are given as $\tau_1 = 0.389613 - 0.920979i$ and $\tau_2 = 0.389613 + 0.920979i$ with $|\tau_1| = |\tau_2| = 1$. Moreover, bifurcation diagrams and maximum Lyapunov exponents (MLE) of system are depicted in Fig. 15. At the end of this section, we again demonstrate validity of chaos control methods related to Neimark-Sacker bifurcation. For this, first we see the effectiveness of hybrid control method. Assume that $k = 350$, $a = 50.23$, $d = 0.9$, $b = 0.4$ and $c = 0.9$ are substituted in system (5.2). A variation in controllability interval is observed with variation of bifurcation parameter r in chaotic region $[295.294, 380]$. Due to this variation, it is observed that length of controllability interval can be increased by

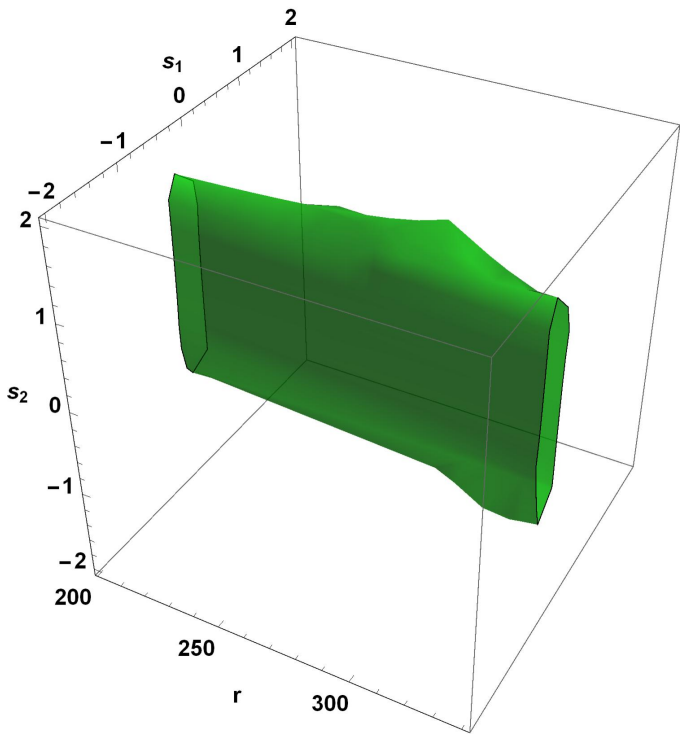

FIGURE 14. For $a = 88.14$, $b = 0.5$, $c = 0.7$, $d = 150$ and $k = 500$ controllability region of system (5.4).

shifting the value of bifurcation parameter at the left end of chaotic region. Variation of controllability with respect to control parameter r is distributed in Fig. 16 in $r\alpha$-plane. From Fig. 16, it is clear that hybrid control method is more effective for controlling chaotic behavior in system (1.2) under the influence of Neimark-Sacker bifurcation, whereas in case of period-doubling bifurcation its chaos controlling speed is slow. Finally, to see the effectiveness of exponential type control strategy, we choose $k = 350$, $a = 50.23$, $d = 0.9$, $b = 0.4$ and $c = 0.9$ for system (5.4). For these selected values and $r \in [295.294, 380]$, the controllability region of system (5.4) is depicted in Fig. 17 in rs_1s_2-space.

Concluding remarks

In the list of complex dynamics, interaction of larch budmoth in Swiss Alps has remained one of the best topic for investigation with respect to both theoretical and experimental point of views. During such interaction, remarkable regular oscillations are observed, and moth population fluctuates up to surprising extent of densities during a particular cycle [11]. Taking into account the interaction between budmoth and quality of larch trees located in the Swiss Alps, a two-dimensional discrete system is proposed and studied in this paper. The Ivlev type functional response concerning the plant quality is replaced to its better nonlinear approximation. Due to implementation of such nonlinear approximation, proposed model shows excellent agreement

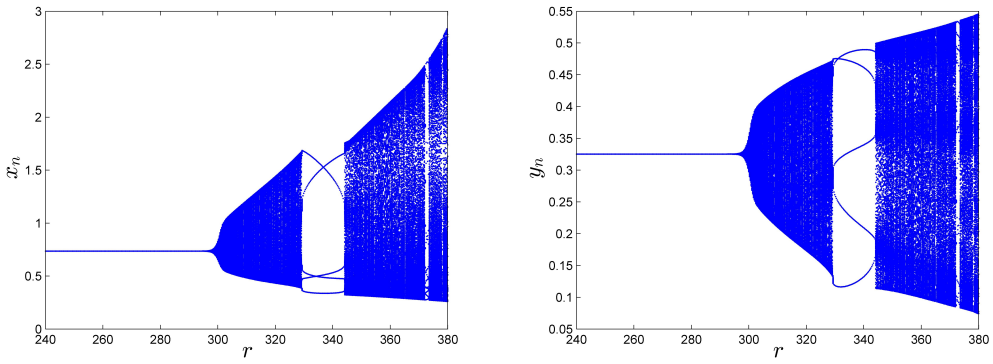

(A) Bifurcation diagram for x_n (B) Bifurcation diagram for y_n

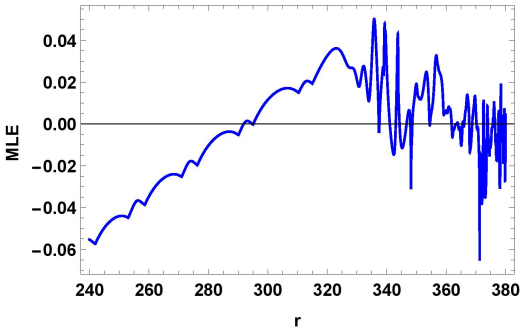

(C) Maximum Lyapunov exponents

FIGURE 15. Bifurcation diagrams and MLE for system (1.2) with $k = 350$, $a = 50.23$, $d = 0.9$, $b = 0.4$, $c = 0.9$, $r \in [240, 380]$ and $(x_0, y_0) = (0.7357,\ 0.325)$.

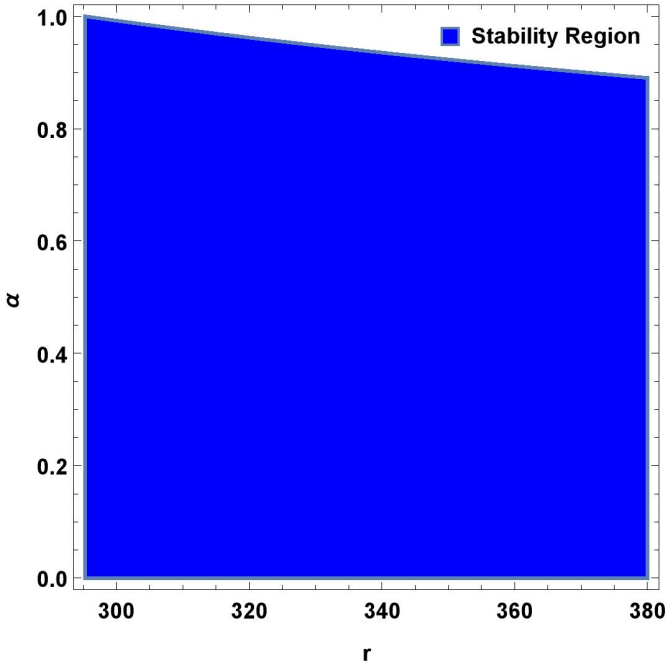

FIGURE 16. For $k = 350$, $a = 50.23$, $d = 0.9$, $b = 0.4$, $c = 0.9$ and $r \in [295.294, 380]$ controllability region of system (5.2).

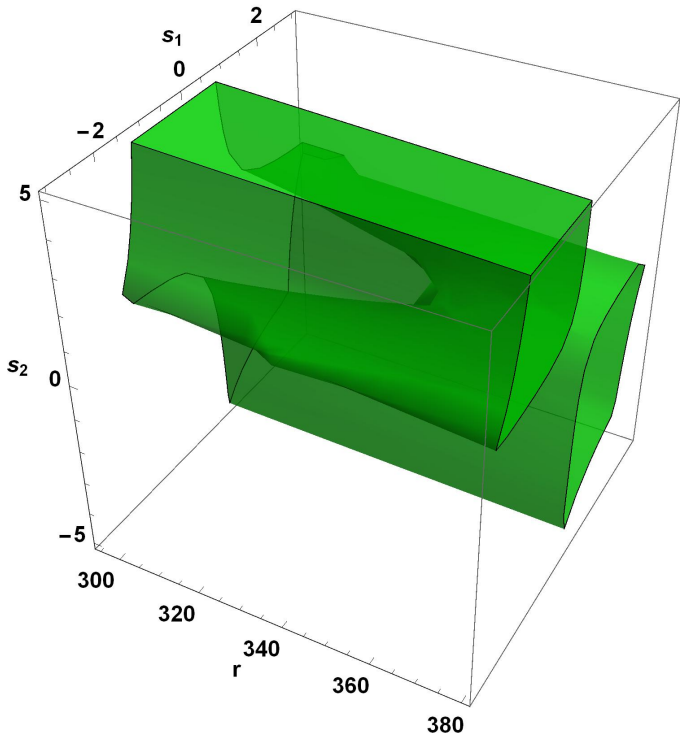

FIGURE 17. For $k = 350$, $a = 50.23$, $d = 0.9$, $b = 0.4$, $c = 0.9$ and $r \in [295.294, 380]$ controllability regions of system (5.4).

with field and experimental data. Furthermore, mathematical analysis related to existence of positive fixed point in closed form, stability and bifurcation analysis are more appropriate for this proposed model. We investigate qualitative aspects of this discrete-time system for interaction between budmoth and quality of larch trees. Boundedness of solutions, existence of fixed points and their topological classification is carried out. It is proved that system experiences period-doubling bifurcation at its positive fixed point with utilizing center manifold theorem and normal forms theory. Moreover, existence and direction for torus bifurcation are also investigated for larch budmoth interaction. Bifurcating and fluctuating behaviors of system are controlled through utilization of three chaos control strategies. Our study reveals that OGY method is unable to control fluctuating and chaotic behavior of model under the influence of both bifurcations. On the other hand, hybrid control method and chaos control strategy of exponential type are remarkably effective for both types of bifurcations.

REFERENCES

[1] L. R. Ginzburg, D. E. Taneyhill, Population cycles of forest Lepidoptera: a maternal effect hypothesis, J. Anim. Ecol., 63(1994), 79–92.

[2] J. H. Myers, Can a general hypothesis explain population cycles of forest Lepidoptera?, Adv. Ecol. Res., 18(1988), 179–242.

[3] B. Wermelinger, B. Forster, D. Nievergelt, Cycles and importance of the larch budmoth, WSL Fact Sheet, 61(2018), 1-12.

[4] C. Zimmer, Life after chaos, Science, 284(1999), 83–86.

[5] J. Esper, U. Buntgen, D. C. Frank, D. Nievergelt, A. Liebhold, 1200 years of regular outbreaks in alpine insects, Proc. R. Soc. London, Ser. B, 274(2007), 671–679.

[6] O. Konter, J. Esper, A. Liebhold, T. Kyncl, L. Schneider, E. Duthorn, U. Buntgen, Tree-ring evidence for the historical absence of cyclic larch budmoth outbreaks in the Tatra Mountains, Trends. Ecol. Evol., 29(2015), 809–814.

[7] W. Baltensweiler, A. Fischlin, The larch budmoth in the Alps, in: A. Berryman (Ed.), Dynamics of Forest Insect Populations: Patterns, Causes, Implications, Plenum, New York, (1988), pp. 331-351.

[8] W. Baltensweiler, Why the larch bud-moth cycle collapsed in the subalpine larch-cembran pine forests in the year 1990 for the first time since 1850, Oecologia, 94(1993), 62–66.

[9] A. A. Berryman, What causes population cycles of forest Lepidoptera?, Trends. Ecol. Evol., 11(1996), 28–32.

[10] G. Battipaglia *et al.*, Long-term effects of climate and land-use change on larch budmoth outbreaks in the French Alps, Clim. Res., 62(2014), 1–14.

[11] P. Turchin, Complex Population Dynamics, Princeton University Press, New Jersey, (2003).

[12] S. R.-J. Jang, D. M. Johnson, Dynamics of discrete-time larch budmoth population models, J. Biol. Dynam., 3(2009), 209–223.

[13] S. R.-J. Jang, J.-L.Yu, Models of plant quality and larch budmoth interaction, Nonlinear Anal. Theory Methods Appl., 71(12)(2009), e1904–e1908.

[14] T. M. M. De Silva, S. R.-J. Jang, Period-doubling and Neimark-Sacker bifurcations in a larch budmoth population model, J. Differ. Equ. Appl., 23(10)(2017), 1619–1639.

[15] S. V. Iyengar, J. Balakrishnan, J. Kurths, Impact of climate change on larch budmoth cyclic outbreaks, Sci. Rep., 6(2016): 27845.

[16] J. Balakrishnan, S. V. Iyengar, J. Kurths, Missing cycles: Effect of climate change on population dynamics, Indian Academy of Sciences Conference Series, 1(1)(2017), 93–99.

[17] I. Ali, U. Saeed, Q. Din, Bifurcation analysis and chaos control in a discrete–time plant quality and larch budmoth interaction model with Ricker equation, Math. Meth. Appl. Sci., 42(18)(2019), 7395–7410.

[18] W. Baltensweiler, U. M. Weber, P. Cherubini, Tracing the influence of larch–bud–moth insect outbreaks and weather conditions on larch tree–ring growth in Engadine (Switzerland), Oikos, 117(2008), 161–172.

[19] , M. P. Hassell, J. H. Lawton, J. R. Beddington, Sigmoid functional responses by invertebrate predators and parasitoids, J. Anim. Ecol., 46(1977), 249–262.

[20] X. Yang, Uniform persistence and periodic solutions for a discrete predatorprey system with delays, J. Math. Anal. Appl., 316(2006), 161-177.

[21] J. Carr, Application of Center Manifold Theory, Springer–Verlag, New York, (1981).

[22] J. Guckenheimer, P. Holmes, Nonlinear Oscillations, Dynamical Systems, and Bifurcations of Vector Fields, Springer–Verlag, New York, (1983).

[23] C. Robinson, Dynamical Systems: Stability, Symbolic Dynamics and Chaos, Boca Raton, New York, (1999).

[24] S. Wiggins, Introduction to Applied Nonlinear Dynamical Systems and Chaos, Springer–Verlag, New York, (2003).

[25] Y. H. Wan, Computation of the stability condition for the Hopf bifurcation of diffeomorphism on R^2, SIAM. J. Appl. Math., 34(1978), 167–175.

[26] Y. A. Kuznetsov, Elements of Applied Bifurcation Theory, Springer-Verlag, New York, (1997).

[27] Q. Din, Stability, bifurcation analysis and chaos control for a predator-prey system, J. Vib. Control, 25(3)(2019), 612-626.

[28] Q. Din, M. S. Shabbir, M. A. Khan, K. Ahmad, Bifurcation analysis and chaos control for a plant-herbivore model with weak predator functional response, J. Biol. Dyn., 13(1)(2019), 481–501.

[29] M. A. Abbasi, Q. Din, Under the influence of crowding effects: stability, bifurcation and chaos control for a discrete–time predator-prey model, Int. J. Biomath., 12(04)(2019): 1950044.

[30] Q. Din, M. Hussain, Controlling chaos and Neimark–Sacker bifurcation in a host–parasitoid model, Asian J. Control, 21(3)(2019), 1202–1215.

[31] Q. Din, M. A. Iqbal, Bifurcation analysis and chaos control for a discrete-time enzyme model, Z. Naturforsch. A, 74(1) (2019), 1-14.

[32] W. Ishaque, Q. Din, M. Taj, M. A. Iqbal, Bifurcation and chaos control in a discrete-time predator-prey model with nonlinear saturated incidence rate and parasite interaction, Adv. Differ. Equ., 2019(2019): 28.

[33] E. M. Elsayed, Q. Din, Period-doubling and Neimark-Sacker bifurcations of plant-herbivore models,Adv. Differ. Equ., 2019(2019): 271.

[34] Q. Din, A novel chaos control strategy for discrete-time Brusselator models, J. Math. Chem., 56(10)(2018), 3045-3075.

[35] Q. Din, Bifurcation analysis and chaos control in discrete-time glycolysis models, J. Math. Chem., 56(3)(2018), 904-931.

[36] Q. Din, T. Donchev, D. Kolev, Stability, Bifurcation Analysis and Chaos Control in Chlorine Dioxide-Iodine-Malonic Acid Reaction, MATCH Commun. Math. Comput. Chem., 79(3)(2018), 577-606.

[37] Q. Din, U. Saeed, Bifurcation analysis and chaos control in a host-parasitoid model, Math. Method Appl. Sci., 40(14)(2017), 5391–5406.

[38] Q. Din, A. A. Elsadany, H. Khalil, Neimark-Sacker bifurcation and chaos control in a fractional-order plant-herbivore model, Discrete Dyn. Nat. Soc., 2017(2017): 6312964.

[39] Q. Din, Qualitative analysis and chaos control in a density-dependent host-parasitoid system, Int. J. Dynam. Control, 6(2)(2018), 778-798.

[40] Q. Din, Neimark-Sacker bifurcation and chaos control in Hassell-Varley model, J. Differ. Equations Appl., 23(4)(2017), 741-762.

[41] Q. Din, O. A. Gumus, H. Khalil, Neimark-Sacker Bifurcation and Chaotic Behaviour of a Modified Host-Parasitoid Model, Z. Naturforsch. A, 72(1)(2017), 25-37.

[42] E. Ott, C. Grebogi, J. A. Yorke, Controlling chaos, Phys. Rev. Letters, 64(11)(1990), 1196–1199.

[43] X. S. Luo, G. R. Chen, B. H. Wang, J. Q. Fang, Hybrid control of period–doubling bifurcation and chaos in discrete nonlinear dynamical systems, Chaos Soliton Fract., 18(4)(2003), 775–783.